



ELSEVIER

Journal of Molecular Structure (Theochem) 371 (1996) 171–183

THEO
CHEM

Analysis of the changes on the potential energy surface of Menshutkin reactions induced by external perturbations^{1,2}

X. Fradera, Ll. Amat, M. Torrent, J. Mestres, P. Constans, E. Besalú, J. Martí, S. Simon, M. Lobato, J.M. Oliva, J.M. Luis, J.L. Andrés, M. Solà, R. Carbó*, M. Duran

Institut de Química Computacional and Departament de Química, Universitat de Girona, 17071 Girona, Catalonia, Spain

Received 13 February 1996; accepted 21 March 1996

Abstract

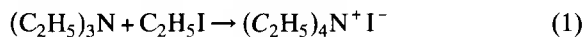
A quantitative analysis of the changes induced by solvation and static uniform electric fields on the potential energy surface of the S_N2 Menshutkin-type reaction between ammonia and methyl chloride has been performed with the help of different indexes. These indexes have been defined to account for the structural and electronic degree of advance of the transition state with respect to the reactant complex and ion pair product through the use of geometrical parameters, dipole moments and electron density distributions. Indexes reveal that external perturbations yield transition states which are both electronically and structurally advanced as compared to the transition state in the gas phase. The overall study is complemented with HOMO–LUMO orbital considerations, quantification of the global charge density redistributions by means of quantum molecular self-similarity measures and an analysis of the topological features of electron density distributions.

Keywords: Menshutkin reaction; solvent effects; uniform electric fields; electron density redistributions; quantum molecular similarity measures

1. Introduction

Menshutkin's landmark study [1,2] on the second-order rate constant for the quaternization of triethylamine with ethyl iodide (Eq. (1)) using 22 solvents, is one of the first systematic analyses of solvent effects on reaction rates. These studies pointed out for the

first time that the polarity of the solvent can modify dramatically the reaction rate.



Since Menshutkin's original work, there has been a large number of experimental studies aiming to rationalize and estimate the possible changes in transition state (TS) structures induced by different solvents, nucleophiles and leaving groups. A recent and extensive review of experimental data referred to Menshutkin's reaction (MR) can be found in Ref. [3]. Analyses of experimental kinetic data, which have been more indicative rather than conclusive, have been usually performed within the framework of transition state theory [4], followed by

* Correspondence may be sent to R. Carbó or M. Duran.

¹ The Institute of Computational Chemistry of the University of Girona dedicates this contribution to Prof. Juan Bertrán on the occasion of his 65th birthday and in recognition of his distinguished and pioneering works on the analysis of chemical kinetics and molecular dynamics in the presence of electric fields and in solution.

² J. Mestres, E. Besalú, J. Martí, J.L. Andrés, M. Solà and M. Duran are former graduate students of Prof. Bertrán.

Brønsted–Hammett treatments [5,6]. The results obtained have been interpreted in the light of the predictions made by Leffler–Hammond [7], Thornton [8] and Kurz [9].

The MR is a special type of S_N2 reaction [10], where the reactants are neutral, as opposed to most usual S_N2 reactions, where one of the reactants is charged. Thus, while along the reaction coordinate of usual S_N2 reactions there is a charge migration, in MRs there is a creation of two ions of opposite sign, followed by their separation. This process is extremely unfavourable in the gas phase due to attractive Coulombic interactions. Indeed to date, only an experimental study on MRs in the gas phase has been reported [11], where crossed molecular beams were used to study the dynamics of the MRs between different alkyl iodides and quinuclidine, pyridine and tri-*n*-propylamine. These results [11] suggest that, on the reactant side, the covalent surface is lower than the ionic surface and that it is relatively flat until the reactants meet. After that, it becomes repulsive. On the product side, the ionic surface is lower in energy and it is strongly attractive due to the Coulomb attraction between the ions. The reaction has been interpreted in terms of covalent and ionic curves crossing and a harpoon-like mechanism.

The situation in the gas phase changes dramatically in the presence of the solvent. In solution, exothermicity [12], sensitivity to steric effects [12] and inverse α -deuterium isotope effects [13] for this reaction were found to be consistent with a crowded TS in which bond making between the nucleophile and the alkyl group is more advanced than bond breaking between the alkyl group and the halide. As expected, it is found [12] that most of the influence of the solvent on the MR is exerted on the TS and the products rather than on the reactants.

These experimentally observed effects and also some specific features of the MRs have been put forward through computational studies [14–21]. Among these works, the investigation by Bertrán et al. [16] was the first to introduce solvent effects in a theoretical study of a MR. In particular, that work analyzed solvent intervention in the reaction between ammonia and methyl bromide. Their main results, confirmed by subsequent research [17–21], revealed that when going from the gas phase to

solution there is: first, a progressive stabilization of the chemical system along the reaction coordinate, which translates into an increased exothermicity; second, an advance of the TS along the reaction coordinate in agreement with the Leffler–Hammond postulate [7]; and third, a polarization of the solute due to the reaction field which leads to a charge transfer that, with respect to the gas phase, favours the reaction. All these features of MRs were rationalized by a Shaik-type state correlation diagram [16,22].

Therefore, as shown by Bertrán et al. [23] in different studies, solvation is able to modify extensively the potential energy surface (PES) of some reactions. This is especially true in the case of MRs. From the energetic and structural points of view, the TS of MRs in solution is found earlier along the reaction coordinate. On the other hand, from an electronic point of view, since the electronic structure of TSs in the gas phase and in solution contains similar contributions of reactant and product configurations [3,16,20], the TS does not vary too much with solvation. This last fact explains the success of Kirkwood's equation [24,25] in MRs as incorporated into transition state theory, i.e. in solution the TS becomes energetically and structurally reactant-like, whereas with respect to charge transfer remains product-like [3,16,20]. Experimentally, there is also some controversy about the nature of the TS in MRs [3,12,13,26].

The aim of the present work is to discuss the advance of the TS along the reaction coordinate of a MR due to external perturbations through use of different indexes that quantify the “earliness” of the TS with respect to parameters like the geometry, dipole moments and electron density distributions. Changes in electron density distributions can be quantified through use of quantum molecular similarity measures (QMSM) [27–32]. It has been shown that QMSMs are especially well-suited to accurately quantify the advance of the TS along the reaction coordinate in an unambiguous way [27] and, for this reason, they will be used in the present work. Finally, the effect of external perturbations on the electron density of the stationary points is also analyzed with the help of HOMO–LUMO orbital analysis, electron density difference maps [33] and Bader's analysis of the topological features of electron density distributions [34].

2. Methodological details

Since the main characteristics of the reaction between ammonia and methyl chloride are similar to those between ammonia and methyl bromide or methyl iodide [19], for computational reasons we have selected the former reaction as a model for the study of MRs. The C_{3v} symmetry of the MR between H_3N and CH_3Cl was maintained during the geometry optimizations. The three heavy atoms, N, C and Cl, were constrained to be collinear along the C_3 symmetry axis. It can be safely assumed that evolution from reactants to the TS is linear. In fact, the intrinsic reaction path (IRP) for the $H_3N + CH_3Br$ MR confirmed the connection between linear structures of the reactant complex, transition state and ion pair product [16]. Nevertheless, it must be noted that a nonlinear ion pair product has been found to be more stable than the linear structure [19]. This nonlinear ion pair product is stabilized by the formation of a hydrogen bond between the halide ion and one of the hydrogen atoms of the ammonium group.

Wave functions for the different species have been computed at the ab initio Hartree–Fock (HF) and second order Møller–Plesset (MP2) levels using the termed 3-21+G^(*) [35] basis set. In this basis set diffuse functions are included for C, N and Cl, while a polarization function is only considered for second row atoms, i.e. Cl. Stationary points in the gas phase and in the presence of electric fields have been fully optimized under the symmetry restrictions mentioned above. To analyze the changes of the PES in solution, at each point of the IRP computed in vacuo, the effect of solvation has been included in terms of Gibbs energy of solvation by means of the self-consistent reaction field (SCRf) method developed by Miertuš, Scrocco and Tomasi [36]. In this way, we have located in an approximate but reliable manner the stationary points in the PES modified by the solvent.

The reactant-like or product-like character at each point on a PES is usually assigned depending on the sign of a structural reaction coordinate (q) parameter which, in this particular case, is defined as

$$q_i = \frac{(\mathbf{r}_{C-Cl} - \mathbf{r}_{N-C})_i - (\mathbf{r}_{C-Cl} - \mathbf{r}_{N-C})_{TS}^{\text{gas phase}}}{(\mathbf{r}_{C-Cl} + \mathbf{r}_{N-C})_i}, \quad (2)$$

where the TS in the gas phase has been taken as the reference point to define the reaction coordinate at any

point i on the PES. Assuming that variations of \mathbf{r}_{C-Cl} and \mathbf{r}_{N-C} are the most important structural changes as the reaction goes through, the $\mathbf{r}_{C-Cl} - \mathbf{r}_{N-C}$ difference is a good approximation to the global reaction coordinate involving the change of the full set of geometrical parameters.

In order to quantify the reactant-like or product-like character of the TS we have defined three indexes that are used to reflect the proximity of the TS to the reactant complex and ion pair product complexes based on geometrical parameters, dipole moments and electron density distributions. These indexes take values that lie in a range of $[-1,1]$. If the TS is closer to the reactant complex than to the ion pair product the index is negative (but positive otherwise).

On this basis, a structural proximity index (β^s) has been defined as

$$\beta^s = 2 \frac{q_{TS} - q_{RC}}{q_{IPP} - q_{RC}} - 1 \quad (3)$$

where q is computed through Eq. (2). Accordingly, an electronic proximity index (β^e) is defined by the expression

$$\beta^e = 2 \frac{\mu_{TS} - \mu_{RC}}{\mu_{IPP} - \mu_{RC}} - 1 \quad (4)$$

μ being the dipole moment of the species considered.

Finally, an electron density proximity index (β^d) can be derived following the definition due to Cioslowski [37] as

$$\beta^d = \frac{d_{RC,TS} - d_{IPP,TS}}{d_{RC,IPP}} \quad (5)$$

In this expression, $d_{A,B}$ is the euclidean distance between A and B molecular electronic distributions [28], expressed as

$$d_{A,B} = [Z_{A,A} + Z_{B,B} - 2Z_{A,B}]^{1/2} \quad (6)$$

In Eq. (6), $Z_{A,B}$ is the QMSM between species A and B [28]. If A and B have electron densities $\rho_A(\mathbf{r})$ and $\rho_B(\mathbf{r})$, their QMSM is given by the expression

$$Z_{A,B} = \int \rho_A(\mathbf{r}) \rho_B(\mathbf{r}) d\mathbf{r} \quad (7)$$

The value $Z_{A,B}$ depends on the relative spatial orientation of molecular electron distributions $\rho_A(\mathbf{r})$ and $\rho_B(\mathbf{r})$. Therefore, the electron distribution $\rho_B(\mathbf{r})$ must

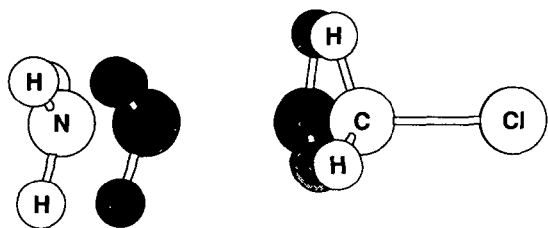


Fig. 1. Relative position of the gas phase reactant complex and transition state which maximizes their quantum molecular similarity measure.

be moved with respect to $\rho_A(\mathbf{r})$ in order to maximize the $Z_{A,B}$ value. For instance, Fig. 1 depicts the relative position between the gas phase reactant complex and TS that maximizes their QMSM. In Fig. 1, the chlorine atoms of the TS and the reactant complex are perfectly superimposed, since the main contribution to the final $Z_{A,B}$ value comes from the overlap between the two chlorine atoms. For a given charge distribution A , the $Z_{A,A}$ value represents its quantum molecular self-similarity measure (self-QMSM). This appears to be an interesting molecular descriptor, because it has been recently shown that this self-QMSM is a measure of how concentrated the electron density is in this particular density distribution [38]. Definitions more general than that of Eq. (7) have been also proposed, based on n th-order density matrices [29].

The computation of wave functions and electron densities was performed with the help of the GAUSSIAN 94 program [39]. The gas phase IRP was constructed using the GAMESS program [40] going downhill from the TS in mass-weighted cartesian coordinates [41]. Calculations of exact and atomic shell approximated (ASA) [42] QMSM were done by means of the ASAC program [43]. All reported QMSM are exact, although for computational reasons, optimizations of the relative spatial orientation of the two molecules in QMSM calculations were carried out using ASA-QMSM. Under this approximation, electron densities in Eq. (7) are expressed as linear combinations of spherical Gaussian functions with all coefficients of the expansion restricted to be positive [42]. Computation of the topological features of electron density distributions (location and characterization of bond critical points) and electron density difference maps were carried out with the program ELECTRA [44].

3. Results and discussion

In this section, the global changes produced on the gas phase PES of the MR by the effect of external perturbations are studied. These effects have been simulated by the application of uniform electric fields (EF) of strengths 0.001 and 0.005 au ($1 \text{ au} = 5.14218 \times 10^{11} \text{ V m}^{-1}$) and by a continuum solvent model using dielectric constants of 1.88 (*n*-hexane) and 78.36 (water). The changes which occurred on the structures and energies and on the electronic density distributions of the stationary points will be analyzed separately.

3.1. Analysis of the structural and energetic changes

Table 1 gathers the main structural parameters (the r_{N-C} and r_{C-Cl} distances and the $\angle H_CCN$ angle) of the five stationary points together with the relative energies with respect to reactants at the gas phase and when external perturbations were applied. Also included are those values derived from the structural parameters: which can be called the structural skeleton of each stationary point ($r_{N-C} + r_{C-Cl}$), the structural reaction coordinate (q) and the structural proximity index (β^s).

Referring first to energetic considerations, the gas phase energy profile for the studied MR is shown in

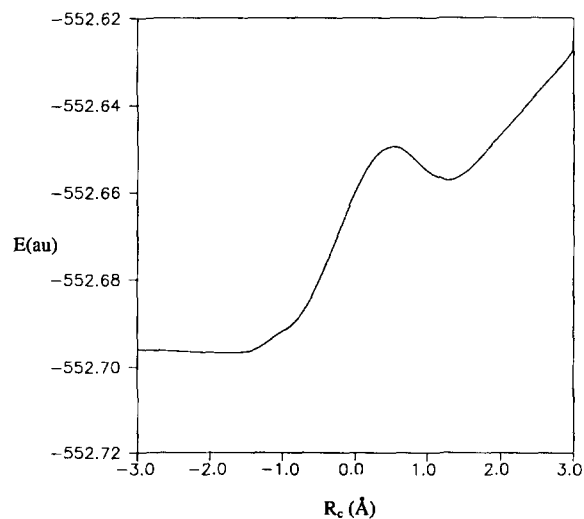


Fig. 2. Energy profile for the MR between H_3N and CH_3Cl in the gas phase.

Table 1

Values of the most important geometric parameters, structural reaction coordinate (q), structural skeleton distance ($r_{C-Cl} + r_{N-C}$), structural proximity index (β^s) and relative energies referred to separated reactants, for the different external perturbations considered. The gas phase MP2 results are given in parentheses. Distances in Å, angles in degrees and energy differences in kcal mol⁻¹

Species	r_{N-C}	r_{C-Cl}	$\angle H_CCN$	$r_{C-Cl} + r_{N-C}$	q	β^s	ΔE^a
Gas phase							
R	∞	1.806					0.0
	(∞)	(1.816)					(0.0)
RC	3.596	1.813	71.7	5.409	-0.426		-1.9
	(3.488)	(1.822)	(71.5)	(5.310)	(-0.439)		(-2.5)
TS	1.932	2.451	95.5	4.383	0.000	0.434	27.8
	(1.866)	(2.459)	(97.7)	(4.325)	(0.000)	(0.551)	(27.3)
IPP	1.599	2.868	107.1	4.466	0.168		22.9
	(1.625)	(2.778)	(106.7)	(4.403)	(0.127)		(25.2)
P	1.545	∞	107.8				102.0
	(1.559)	(∞)	(107.7)				(106.5)
$f = 0.001$							
R	∞	1.808					0.0
RC	3.564	1.816	71.8	5.380	-0.421		-2.1
TS	1.958	2.435	94.6	4.393	-0.010	0.379	25.5
IPP	1.593	2.896	107.3	4.489	0.175		19.4
P ^b	1.546	∞	107.8				62.1
$f = 0.005$							
R	∞	1.817					0.0
RC	3.456	1.829	72.0	5.285	-0.406		-2.5
TS	2.054	2.378	91.8	4.432	-0.044	0.189	17.2
IPP	1.576	3.029	107.8	4.605	0.203		5.14
TS	1.547	6.410	107.9	7.957	0.611		17.9
P ^b	1.546	∞	107.7				-34.6
$\epsilon = 1.88$							
R	∞	1.806					0.0
RC	3.596	1.813	71.7	5.409	-0.426		-1.7
TS	2.060	2.350	90.6	4.410	-0.052	0.201	24.1
IPP	1.584	3.007	107.8	4.591	0.197		8.5
P	1.546	∞	107.8				27.0
$\epsilon = 78.36$							
R	∞	1.806					0.0
TS	2.242	2.199	83.9	4.441			20.7
P	1.546	∞	107.8				-55.7

^a The reference energies are: $E_{\text{gas phase}} = -552.6937$ au, $E_{f=0.001} = -552.6952$ au, $E_{f=0.005} = -552.7022$ au, $E_{\epsilon=1.88} = -552.6971$ au, $E_{\epsilon=78.36} = -552.7045$ au.

^b Ionic products separated by 20 Å.

Fig. 2. This is the well-established asymmetric double-well potential with five stationary points, corresponding to separated reactants (R), the dipole–dipole reactant complex (RC), the transition state (TS), the ion pair products (IPP) and finally the separated ionic products (P). This highly endothermic energy profile is consistent with experimental data obtained from crossed molecular beams [11]. The

HF gas phase calculated reaction energy of 102.0 kcal mol⁻¹ does not differ much from the experimental value of 110 ± 5 kcal mol⁻¹ [17] obtained from the standard Gibbs energies of formation of reactants and products. Inclusion of correlation energy by means of the MP2 method improves the gas phase reaction energy yielding 106.5 kcal mol⁻¹, although it does not alter the general picture of the

asymmetric double-well potential observed at the HF level and, therefore, it validates the results obtained at this level of theory.

As can be extracted from ΔE values in Table 1, the shape of the gas phase double-well energy profile is substantially changed when an external perturbation is applied. In general, the energy barrier at the TS diminishes and the exothermicity of the reaction increases. Comparing the effects of applying an EF or a continuum solvent model, the simulated solvent effect due to *n*-hexane is found to be midway between the two selected EF strengths, both from the TS energy barrier and the exothermicity of the process. Interestingly, in water solution the reaction is exothermic by $-55.7 \text{ kcal mol}^{-1}$, which means that the ionic products have been stabilized by $157.7 \text{ kcal mol}^{-1}$ with respect to the gas phase reaction. This value is not far from the experimental standard Gibbs energy of the MR between ammonia and methyl chlorine in water which is $-34 \pm 10 \text{ kcal mol}^{-1}$ and the $-37 \pm 2 \text{ kcal mol}^{-1}$ obtained with Monte Carlo statistical calculations [17]. Further, the energy barrier of $20.7 \text{ kcal mol}^{-1}$ agrees with the experimental activation barrier of $23.5 \text{ kcal mol}^{-1}$ for the MR between ammonia and methyl iodide in water [45]. This represents a lowering of the gas phase barrier height by $9.0 \text{ kcal mol}^{-1}$ caused by hydration. Thus it seems that, as far as energetic considerations are concerned, both theoretical models of the introduction of the effect of external perturbations are able to qualitatively reproduce the observed experimental facts.

With respect to the HF and MP2 gas phase structural parameters, it is interesting to note that, along the reaction coordinate, the increase of the $r_{\text{N-Cl}}$ bond length and the decrease of the $r_{\text{N-C}}$ distance is followed by the typical umbrella inversion about the carbon atom, as revealed by the opening of the $\angle \text{H}_c\text{CN}$ angle. At the TS, the umbrella inversion is almost completed, the C–Cl bond is fairly broken and the C–N bond is partially formed, the Pauling bond orders [46] for these bonds being 0.116 and 0.275, respectively, at the HF level. These facts provide us a first clue on the structural product-like nature of the gas phase TS. This statement is reinforced by the $r_{\text{C-Cl}} - r_{\text{N-C}}$ value in the gas phase TS which is 0.519 \AA at the HF level and 0.593 \AA at the MP2 level. For the sake of comparison with the structures obtained when an external perturbation is applied, the structural

reaction coordinate (q) was standardized with respect to this value (Eq. (2)), so it becomes zero for the TS point at the gas phase. Furthermore, the structural proximity of the process is clearly unbalanced to the product site, as derived from the positive value of β^s . On the other hand, another aspect that supports the structural product-like nature of the TS at the gas phase is the structural skeleton of the different stationary points along the reaction coordinate. For this particular reaction, it is found that the structural skeleton is remarkably compressed when going from the RC to the TS (see Table 1) while it is kept almost constant when going downhill to the IPP. All these structural considerations are in accordance with the Leffler–Hammond [7] postulate, due to the energetic proximity of TS and IPP. For the EF of 0.005 au, besides the TS corresponding to the MR, we have located another TS between the IPP and the ionic products, corresponding to the overcoming of Coulombic interactions between the two created ions of opposite sign.

As regards the structural changes occurring upon solvation when compared to the gas phase process, the most relevant result turns out to be the fact that, on the structural reaction coordinate, RC and IPP are both delayed (i.e. more product-like), while the TS is advanced (i.e. more reactant-like). For the sake of clarity, this general trend of external perturbation effects on the structure of the different stationary points has been qualitatively depicted in Scheme 1. This result is confirmed from the inspection of q values, which ultimately reflect the changes on $r_{\text{N-C}}$ and $r_{\text{C-Cl}}$ distances. Thus, for RC and IPP, more positive q values are obtained while slight negative q values emerge for TS. Closely related to this is the fact that, under the effect of external perturbations, the process experiences an important gain in its structural proximity, as derived from the smaller values.

Another aspect that deserves special mention in this case is the evolution of the so-called structural skeleton ($r_{\text{N-C}} + r_{\text{C-Cl}}$) under the effect of an external perturbation. It is found that, while RC is compressed, TS and IPP are structurally expanded, the TS being the tightest species along the reaction coordinate. From the ensemble of this consideration and the above-mentioned structural trends, a question arises on which can be considered the reference structural point on the reaction coordinate or, in other words,

“is the TS becoming RC-like?” or should we consider that “is it the RC which is becoming TS-like?” On this question, a recent work [27] reported that the advancement of the TS in the $F^- + CH_3F$ S_N2 reaction under the effect of uniform electric fields can be better explained when considering that the RC is becoming more TS-like, rather than, as usually stated, the TS is becoming more RC-like. In the case of the MR this is not as clear as it was for the $F^- + CH_3F$ S_N2 reaction. Taking as an example, the effect caused by an EF of strength 0.005 au, several factors have to be considered: (i) the internal structural change (measured by Δq) is -0.044 for TS and $+0.020$ for RC, which would be in agreement with the TS becoming more RC-like; (ii) connected with this internal structural change, the $\angle H_CCN$ umbrella angle is substantially altered in the TS while it almost does not change in the RC, which reinforces the idea of the TS becoming more RC-like; however, (iii) from the structural skeleton viewpoint, the TS becomes slightly looser ($+0.049$ Å) while the RC is -0.124 Å compressed. Thus, on this basis, it is the RC which is experiencing the most important evolution. As can be seen, for this particular reaction, both RC and TS approach each

other. However, changes in the geometrical parameters that are more relevant in the definition of the global reaction coordinate (q and $\angle H_CCN$) indicate that the TS becomes RC-like rather than otherwise. This is another aspect that differentiates S_N2 reactions from MRs. It can be rationalized by the Shaik-type state correlation diagram for a MR [16], because the product diabatic curve is much more stabilized than the reactant diabatic curve due the presence of external perturbations, thus leading to a RC which is somewhat delayed and a TS which is quite advanced along the reaction coordinate.

3.2. Analysis of the electronic changes

Table 2 collects the self-QMSMs and dipole moments of the RC, TS and IPP stationary points together with the values of the electronic and electron density proximity indexes for the different external perturbations considered. Also included are the HOMO and LUMO energies and the hardness parameter derived from them.

It has been shown in the last section that the reaction coordinate and the structural proximity index

Table 2

Self-QMSMs (au), dipole moments (au), electronic and electron density proximity parameters, HOMO and LUMO energies (eV), and the hardness parameter in the gas phase and for the electric fields and solvents studied

Species	Z_{AA}	μ	β^e	β^d	ϵ_{HOMO}	ϵ_{LUMO}	η^a
Gas phase							
RC	1058.033	1.73			-0.420	0.098	0.259
TS	1058.073	5.19	0.301	0.204	-0.328	0.022	0.175
IPP	1058.017	7.05			-0.268	-0.006	0.140
$f = 0.001$							
RC	1058.035	1.80			-0.416	0.094	0.255
TS	1058.070	5.14	0.242	0.172	-0.334	0.028	0.181
IPP	1058.011	7.17			-0.288	-0.001	0.143
$f = 0.005$							
RC	1058.038	2.07			-0.398	0.075	0.237
TS	1058.059	4.96	0.034	0.058	-0.354	0.051	0.202
IPP	1057.990	7.66			-0.297	0.016	0.157
$\epsilon = 1.88$							
RC	1058.031	1.73			-0.420	0.098	0.259
TS	1058.089	4.62	-0.012	0.007	-0.349	0.033	0.191
IPP	1057.997	7.58			-0.291	-0.002	0.145
$\epsilon = 78.36$							
TS	1058.079	3.71			-0.379	0.048	0.214

^a $\eta = (E_{LUMO} - E_{HOMO})/2$

indicate the product-like nature of the TS in the gas phase. From an electronic point of view, the gas phase TS has also a product-like character. The Mulliken charge on chlorine is -0.711 au and the value of the electronic proximity index is 0.301 , while the electron density proximity parameter is 0.204 . Such structurally and geometrically “late” TS for this highly endothermic reaction is in agreement with the predictions based on the Leffler–Hammond postulate.

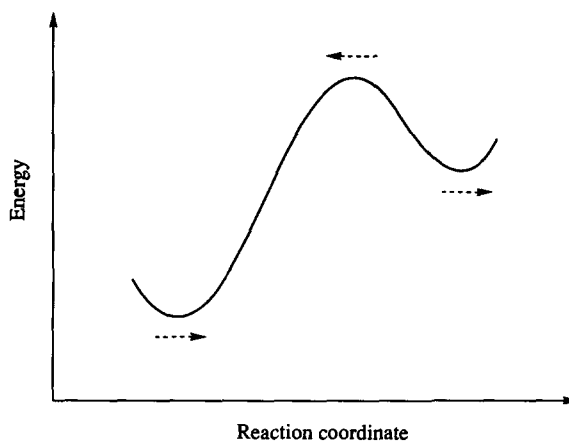
The self-QMSM in the gas-phase TS is the largest one along the reaction coordinate from the RC to the IPP. As mentioned above, the larger the self-QMSM, the higher the electron charge concentration, so a large self-QMSM in the TS is consistent with the picture of a crowded TS. Inspection of the $r_{N-C} + r_{C-Cl}$ values in Table 1 reveals that TS is the tightest species along the reaction coordinate, although it becomes looser with the increase in the strength of the EF applied, whereas the RC becomes tighter. The $Z_{A,A}$ values globally exhibit these two effects: first, self-QMSM for the TS are larger than for the RC, which is related to a larger concentration of electronic charge in the TS; second, for the RC $Z_{A,A}$ increases with the intensity of the EF, while for the TS, $Z_{A,A}$ becomes smaller. In solution, $Z_{A,A}$ values do not exactly follow this second trend. As found above, self-QMSM for the TS in *n*-hexane is larger than that in water. However, both values are larger than in gas phase TS, despite the TS in solution being looser. This fact can be attributed to the special charge redistribution induced by the solvent on each particular side of the complex which, for anionic species, may result in increased self-QMSM [32].

The last section has shown that MRs are catalyzed by the presence of well-oriented EFs and by solvents. Both EFs and solvents act through polarization of the electron density, hence favouring the reaction. However, there is a difference between polarization induced by EFs and that by solvents. The electric field generated by the polarized solvent is known as the reaction field. Interestingly and in contrast to EFs which are kept constant, the reaction field induced by solvents depends on the polarization of the solute and therefore increases along the reaction coordinate. This reaction field exerts a feedback effect leading to further polarization of the solute, which in turn increases the polarization of the solvent. Accordingly, the ionic products originate more intense fields and

therefore are more stabilized by solvents than the reactants.

From an electronic point of view, every point in the IRP becomes more product-like when an external perturbation is applied. Further, the stabilization by external perturbations increases when going from the reactants to the products, due to the increased charge separation. This leads to the consequence that geometrical changes suffered by minima will represent a delay along the reaction coordinate, while changes suffered by maxima will suppose an advancement. Indeed, as shown in the last section, while the RC and the IPP follow the opposite direction, the geometrical changes of the TS follow the direction of advancement (see Scheme 1). This results in a TS with a somewhat advanced electronic distribution as compared to the gas phase TS, despite all points in the IRP being electronically retarded.

This point is confirmed by the charges on the chlorine atom for the TSs, which are -0.711 au in the gas phase, -0.705 and -0.685 au for EFs of 0.001 and 0.005 au, and -0.637 and -0.490 au in solution of *n*-hexane and water. These charges, together with the evolution suffered by the dipole moment values collected in Table 2, show that, from an electronic point of view, the TS is somewhat advanced (i.e. more reactant-like). This is specially true for solvents, since in this case the reaction field increases along the reaction coordinate. On the other hand, electronically, both the RC and particularly the IPP follow the opposite direction and become more product-like.



Scheme 1.

The values for the structural, electronic and electron density proximities at the TSs are 0.379, 0.242 and 0.172 when an EF of 0.001 a.u. is applied, 0.189, 0.034 and 0.058 for an EF of 0.005 au, and 0.201, -0.012 and 0.007 in solution of *n*-hexane. Since the RC is not a stable species in water solution, we have not determined the proximity indexes in this case. As compared to the values for the gas phase (0.434, 0.301 and 0.204), all proximity parameters reflect the electronic and geometrical advancement of the TS with respect to the RC.

Another aspect worth being analyzed is the change in hardness owing to external perturbations. Hardness values [47] have been collected in Table 2 for the RC, the TS and the IPP, and for different external perturbations considered. The principle of maximum hardness (PMH) [47] states that systems with constant chemical potential, temperature and external potential, tend to a state of maximum hardness. Apart from temperature, no restriction imposed by the PMH is accomplished in our system, although Pearson has shown a number of cases [47] in which the PMH is more general and less restrictive. This turns out to be the present case. The RC, which is the most

stable species, has the largest hardness in all cases considered. However, the RC becomes softer with larger EFs, which leads to the RC being more reactive and hence to smaller energy barriers. The opposite trend is observed for the TS and the IPP, which become more stable and, as the PMH asserts, harder with the applied EF. The difference between the hardness of the RC and those of the TS and IPP, diminishes with the increase in the intensity of the EF. Hence, for EFs of enough strength, the hardness of TS and IPP should become larger than the hardness of the RC. One can expect that in this situation, the RC may spontaneously evolve to the IPP. The hardness of the TS in *n*-hexane is intermediate between those corresponding to EFs of 0.001 and 0.005 au, while the TS in water, which is found to be the most stable, has also the larger hardness.

The analysis of the electronic changes induced by the effect of an external perturbation was also carried out from the point of view of the topological features of charge density distributions. Special attention was focused on the two mainly intervening bonds in the transfer of the methyl group, namely, the forming bond (N–C) and the breaking bond (C–Cl).

Table 3

Location from the carbon atom (r , in Å), electron density (ρ , in au), Laplacian of the electron density ($\nabla^2\rho$, in au), and ratio between perpendicular and parallel curvatures ($|\lambda_1/\lambda_3|$) on the N–C and C–Cl bond critical points at reactant complex, transition state, and ion pair product for different uniform electric fields and solvents

Species	r^{N-C}	ρ^{N-C}	$\nabla^2\rho^{N-C}$	$ \lambda_1/\lambda_3 $	r^{C-Cl}	ρ^{C-Cl}	$\nabla^2\rho^{C-Cl}$	$ \lambda_1/\lambda_3 $
Gas phase								
RC	1.7221	0.0038	0.0148	0.1021	0.7149	0.1551	-0.1587	0.8142
TS	0.8171	0.0782	0.1211	0.2668	1.0392	0.0393	0.0932	0.1852
IPP	0.5796	0.1507	0.0158	0.4712	1.2605	0.0176	0.0611	0.0978
$f = 0.001$								
RC	1.7028	0.0041	0.0156	0.1029	0.7144	0.1536	-0.1527	0.8035
TS	0.8328	0.0745	0.1220	0.2593	1.0306	0.0404	0.0930	0.1906
IPP	0.5762	0.1529	0.0092	0.4833	1.2751	0.0167	0.0579	0.0961
$f = 0.005$								
RC	1.6360	0.0050	0.0186	0.1054	0.7137	0.1473	-0.1274	0.7574
TS	0.8877	0.0624	0.1204	0.2352	0.9988	0.0448	0.0928	0.2089
IPP	0.5675	0.1605	-0.0168	0.5295	1.3416	0.0131	0.0444	0.0919
$\epsilon = 1.88$								
RC	1.7222	0.0039	0.0149	0.1034	0.7164	0.1553	-0.1607	0.8178
TS	0.8956	0.0612	0.1300	0.2231	0.9832	0.0478	0.0901	0.2248
IPP	0.5741	0.1585	-0.0199	0.5357	1.3326	0.0139	0.0467	0.0951
$\epsilon = 78.36$								
TS	1.0015	0.0436	0.1263	0.1754	0.9015	0.0652	0.0725	0.3063

Evaluation of the changes which occurred in the electronic nature of these two bonds on each point along the reaction coordinate, was assessed by localizing and characterizing the corresponding bond critical points (BCPs).

Table 3 collects the positions in bonds where the different BCPs are located (\mathbf{r} , distance from the carbon atom), together with their electron density (ρ) and Laplacian ($\nabla^2\rho$) values, and the ratio between the perpendicular and the parallel eigenvalues of the Hessian of the electron density ($|\lambda_1/\lambda_3|$), at the optimized RC, TS and IPP for the different cases studied.

At RCs, the values of ρ , $\nabla^2\rho$ and $|\lambda_1/\lambda_3|$ for the C–Cl bonds are consistent with the existence of an intermediate interaction between these two atoms [34]; the location of the BCPs is closer to the C atom than to the Cl atom and they are characterized by charge density values of about 0.15 au and by negative values of the Laplacian of ca. -0.16 au. The effects of external perturbations on this bond are to approach the position of the BCP still closer to the C atom, to reduce its charge density values and to yield less negative Laplacian values, showing the reduction of the C–Cl bond strength. Also, the $|\lambda_1/\lambda_3|$ ratio is decreased, this result being consistent with the trend of this interaction evolving towards a more ionic interaction. These electronic trends just reflect the structural result that uniform electric fields give larger C–Cl distances at the RC (Table 1).

Moreover, the characteristic values of ρ , $\nabla^2\rho$ and $|\lambda_1/\lambda_3|$ of the BCP for the N–C bond at the RCs show a clear long-range interaction between both atoms; the position of the BCPs is slightly closer to the C atom than to the N atom, the amount of electron density on the BCPs is practically negligible, small positive Laplacian values are found and this results in small $|\lambda_1/\lambda_3|$ values. The effect of an external perturbation on the N–C bond is far less important than it was for the C–Cl bond, because of the large separation and the weak interaction between both atoms, denoting that the main electron density redistribution is taking place on the C–Cl side at this point of the reaction coordinate. In particular, the BCP is translated to a closer position with respect to the C atom and a small amount of electron density on this BCP is appreciated, together with the obtainment of larger $|\lambda_1/\lambda_3|$ values. This electronic behaviour may be in part due

to the structural fact that the RC becomes tighter under the effect of an external perturbation (Table 1).

As the reaction goes through, the situation at the TS differs completely from the one observed at the RC. At this point of the reaction coordinate, closed-shell interactions [34] are established between the C atom and the Cl atom, on one side, and the N atom, on the other side. The relative strength of these two interactions at each particular phase is found to be structurally linked to the distance values obtained for $\mathbf{r}_{\text{N-C}}$ and $\mathbf{r}_{\text{C-Cl}}$ (Table 1); the shorter the distance, the stronger the interaction. The effect of EFs and solvent on this relative strength can be mainly analyzed by comparison of the ρ and $|\lambda_1/\lambda_3|$ values in each case. The general trend is that differences between interactions at both sides of the C atom are reduced under the presence of an EF and even interchanged when solvent effects were introduced. On one side, both ρ and $|\lambda_1/\lambda_3|$ values become larger for the C–Cl interaction (which means weaker closed-shell character), while on the other side these ρ and $|\lambda_1/\lambda_3|$ values become smaller for the N–C interaction (which means stronger closed-shell character). An extreme case is found in water solution where the situation turns out to be electronically completely opposite to that in gas phase.

Finally, as the reaction reaches the IPP, the electronic characteristics of the N–C and C–Cl bonds become interchanged with respect to those observed at RC, in accordance with the structural parameters at this point of the reaction coordinate (Table 1). First, ρ , $\nabla^2\rho$ and $|\lambda_1/\lambda_3|$ values for the BCP of the N–C bond evidence an intermediate interaction between both atoms [34] and second, a long-range interaction is now established between C and Cl atoms. Furthermore, application of an external perturbation tends to reinforce the N–C bond while yielding a weaker C–Cl bond. In this sense, for the BCP in the N–C bond, larger values of ρ and $|\lambda_1/\lambda_3|$ are obtained and negative Laplacian values are developed while contrary to this, for the BCP in the C–Cl bond, smaller values of ρ and $|\lambda_1/\lambda_3|$ are progressively found.

Analysis of the electronic changes on the gas-phase TS structure, when an external perturbation is applied, allows us to understand the electronic redistribution occurring when only electronic relaxation is permitted. Table 4 collects the most important topological features of electron density distributions at the gas phase TS geometry (as presented in Table 3

Table 4

Location from the carbon atom (r , in Å), electron density (ρ , in au), Laplacian of the electron density ($\nabla^2\rho$, in au), and ratio between perpendicular and parallel curvatures ($|\lambda_1/\lambda_3|$) on the N–C and C–Cl bond critical points at the gas phase optimized transition state geometry for different uniform electric fields and solvents. Mulliken charge population on chlorine (in au) is also included

	q_{Cl}	$r^{\text{N-C}}$	$\rho^{\text{N-C}}$	$\nabla^2\rho^{\text{N-C}}$	$ \lambda_1/\lambda_3 $	$r^{\text{C-Cl}}$	$\rho^{\text{C-Cl}}$	$\nabla^2\rho^{\text{C-Cl}}$	$ \lambda_1/\lambda_3 $
Gas phase	-0.711	0.8171	0.0782	0.1211	0.2668	1.0392	0.0393	0.0932	0.1852
$f = 0.001$	-0.722	0.8164	0.0783	0.1188	0.2694	1.0395	0.0391	0.0943	0.1826
$f = 0.005$	-0.765	0.8137	0.0791	0.1094	0.2805	1.0412	0.0382	0.0988	0.1732
$\epsilon = 1.88$	-0.754	0.8134	0.0782	0.1151	0.2717	1.0393	0.0382	0.0979	0.1739
$\epsilon = 78.36$	-0.843	0.8060	0.0783	0.1028	0.2833	1.0721	0.0358	0.1075	0.1522

for the optimized structures), together with the Mulliken atomic charges on chlorine.

As can be observed, when the wave function is allowed to relax under the effect of external perturbations, the charge on the Cl atom increases hence indicating an electronic product-like evolution of the TS. This is exactly opposite to the electronic trend found when the TS at the gas phase was completely reoptimized (i.e. nuclear relaxation was allowed) under the presence of an external perturbation. In this case, the location of the BCPs becomes closer to the Cl atom than to the C atom. Furthermore, the electron density distribution is reorganized to give a slightly reduced interaction between the C and Cl atoms than that obtained from the gas phase electron density distribution, as deduced from the smaller values obtained for ρ and $|\lambda_1/\lambda_3|$, and the more positive Laplacian value. The opposite is true for the N–C bond. Therefore, the external perturbation favours the charge separation and promotes the C–Cl bond breaking and N–C bond formation.

In order to understand how the electron density is being locally redistributed at the TS under the presence of either uniform electric fields or solvents, electron density difference maps have been constructed. In all cases, the gas phase TS optimized geometry is taken as the reference structure and thus no nuclear relaxation is allowed when the external perturbations are applied. Fig. 3 shows the electronic redistribution due to a uniform electric field of 0.005 au (a) and that induced by the effect of a water solution (b). Similar electronic redistributions were obtained when a uniform electric field of 0.001 au and a *n*-hexane solution were considered. As found above, the general trend observed in these two figures is a displacement of the electron density towards the chlorine atom. The main reason for this

redistribution is the reduction in the energy gap between the HOMO of the NH_3 and the LUMO of the CH_3Cl [3] under the effect of external perturbations, which favours the charge transfer. The charge

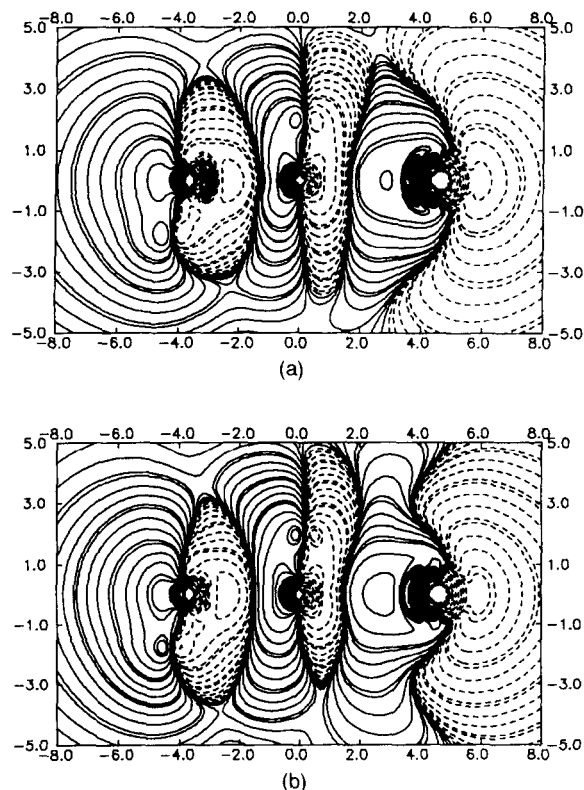


Fig. 3. Difference maps between the electron densities obtained in gas phase and (a) in the presence of a uniform electric field of 0.005 au or (b) in water solution, both at the gas phase optimized transition state geometry. The minimum contour is 1×10^{-5} au and they increase to 2, 4, 8... $\times 10^{-5}$ au. Solid lines correspond to positive values, that is, points where the gas phase electron density is larger. In this map the nitrogen atom is on the left, the carbon atom in the centre, and the chlorine atom on the right.

redistribution increases the electron density in the region of the N–C bond and reduces it in the C–Cl bond, thus favouring the breaking of the C–Cl bond and the formation of the N–C bond, as can be observed in Fig. 3.

4. Conclusions

In this work we have analyzed the effects of uniform electric fields and solvents on the MR between ammonia and methyl chlorine. The discussion has been based on three indexes which give the proximity of the TS to the RC in terms of geometries, dipole moments and electron density distributions.

As compared to usual S_N2 reactions, i.e. S_N2 reactions where one of the reactants is charged, MRs exhibit several significant differences, which arise from the fact that solvent stabilizing effects in MRs are more relevant on the TS and IPP than on the RC. This results in MRs being catalyzed by solvents whereas usual S_N2 reactions are inhibited. Also, in S_N2 reactions changes on RC are more relevant than in the TS, while the opposite is true for MRs.

The gas phase TS of the $NH_3 + CH_3Cl$ MR has a product-like nature, both in structural and electronic terms. External perturbations, like uniform electric fields and solvents, lead to an important stabilization of the products and a significant decrease of the barrier height. From an electronic point of view, every point in the IRP becomes more product-like when an external perturbation is applied. Further, the stabilization by external perturbations increases along the reaction coordinate, due to the increased charge separation. This leads to the consequence that geometrical changes suffered by minima will represent a delay along the reaction coordinate, while changes suffered by maxima will suppose an advance. Indeed, as shown in the last section, while the RC and the IPP follow the opposite direction, the geometrical changes of the TS follow the direction of advance. This results in a TS with a somewhat advanced electronic distribution as compared to the gas phase TS, despite all points on the IRP being electronically delayed.

The overall analysis of the changes induced by external perturbations on the topological features of electron density distributions covers the above-mentioned electronic effect that while RC and IPP

are electronically delayed, the TS is advanced and reduces its original product-like electronic nature.

Acknowledgements

Prof. Bertrán's five former graduate students, J. Mestres, J. Martí, J.L. Andrés, M. Solà and M. Duran, are personally indebted to him for his skilful teaching and continuous encouragement during all these years. Financial help for this work has been provided through the Spanish DGICYT Project No. PB92-0333.

References

- [1] N. Menshutkin, *Z. Phys. Chem.*, 5 (1890) 589.
- [2] N. Menshutkin, *Z. Phys. Chem.*, 6 (1890) 41.
- [3] J.-L.M. Abboud, R. Notario, J. Bertrán and M. Solà, *Prog. Phys. Org. Chem.*, 19 (1993) 1.
- [4] (a) S. Glasstone, K.J. Laidler and H. Eyring, in *The Theory of Rate Processes*, McGraw-Hill, New York, 1941. (b) W.F.K. Wynne-Jones and H. Eyring, *J. Chem. Phys.*, 3 (1935) 493.
- [5] J.N. Brønsted, *Chem. Rev.*, 5 (1928) 231.
- [6] L.P. Hammett, *Chem. Rev.*, 17 (1935) 125.
- [7] (a) S. Hammond, *J. Am. Chem. Soc.*, 77 (1955) 334. (b) J.E. Leffler, *Science*, 117 (1953) 340.
- [8] E.R. Thorton, *J. Am. Chem. Soc.*, 89 (1967) 2915.
- [9] J.C. Harris and J.L. Kurz, *J. Am. Chem. Soc.*, 92 (1970) 349.
- [10] W.L. Hase, *Science*, 266 (1994) 998.
- [11] Y.F. Yen, R.J. Cross and M. Saunders, *J. Am. Chem. Soc.*, 113 (1993) 5563.
- [12] E.M. Arnett and R. Reich, *J. Am. Chem. Soc.*, 102 (1980) 5892.
- [13] J.M. Harris, M.S. Paley and T.W. Prasthofer, *J. Am. Chem. Soc.*, 103 (1981) 5915.
- [14] U. Berg and R. Gallo, *Acta Chem. Scand.*, B37 (1983) 661.
- [15] J.W. Viers, J.C. Schug, M.D. Stovall and J.I. Seeman, *J. Comput. Chem.* 5 (1984) 598.
- [16] M. Solà, A. Lledós, M. Duran, J. Bertrán and J.-L.M. Abboud, *J. Am. Chem. Soc.*, 113 (1991) 2873.
- [17] J. Gao, *J. Am. Chem. Soc.*, 113 (1991) 7796.
- [18] (a) J. Gao and X. Xia, *J. Am. Chem. Soc.*, 115 (1993) 9667. (b) J. Gao and X. Xia, in C.J. Cramer and D.G. Truhlar (Eds.), *Structure and Reactivity in Aqueous Solution*, ACS Symp. Ser. 568, Washington, DC, 1994.
- [19] U. Maran, T.A. Pakkanen and M. Karelson, *J. Chem. Soc., Perkin Trans. 2*, (1994) 2445.
- [20] S. Shaik, A. Ioffe, A.C. Reddy and A. Pross, *J. Am. Chem. Soc.*, 116 (1994) 262.
- [21] U. Berg, M. Chanon, R. Gallo and M. Rajzmann, *J. Org. Chem.*, 60 (1995) 1975.
- [22] S.S. Shaik, *Prog. Phys. Org. Chem.*, 15 (1985) 197.

- [23] (a) J. Bertrán, in J. Bertrán and I.G. Csizmadia (Eds.), *New Theoretical Concepts for Understanding Organic Reactions*, Kluwer, Dordrecht, 1989, pp. 231–255. (b) J. Bertrán, J.M. Lluch, A. González-Lafont, V. Dillet and V. Pérez, *Am. Chem. Soc. Symp. Ser.*, 568 (1994) 168. (c) M. Solà, E. Carbonell, A. Lledós, M. Duran and J. Bertrán, *J. Mol. Struct. (Theochem)*, 255 (1992) 283. (d) J.L. Andrés, A. Lledós, M. Duran and J. Bertrán, *Chem. Phys. Lett.*, 153 (1988) 82. (e) E. Carbonell, J.L. Andrés, A. Lledós, M. Duran and J. Bertrán, *J. Am. Chem. Soc.*, 110 (1988) 996. (f) M. Duran and J. Bertrán, *Rep. Mol. Theory*, 1 (1990) 57. (g) M. Solà, A. Lledós, M. Duran and J. Bertrán, *J. Am. Chem. Soc.*, 114 (1992) 869. (h) M. Solà, A. Lledós, M. Duran and J. Bertrán, *Int. J. Quantum Chem.*, 40 (1991) 511. (i) M. Solà, J.L. Andrés, M. Duran, A. Lledós and J. Bertrán, *Theor. Chim. Acta*, 91 (1995) 333. (j) J.L. Andrés, A. Lledós and J. Bertrán, *Chem. Phys. Lett.*, 223 (1994) 23. (k) J.L. Andrés, M. Duran, A. Lledós and J. Bertrán, *Chem. Phys. Lett.*, 124 (1986) 177.
- [24] J.G. Kirkwood, *J. Chem. Phys.* 2 (1934) 351.
- [25] M.H. Abraham and P.J. Grelhier, *J. Chem. Soc., Perkin Trans. 2*, (1976) 1735.
- [26] D.N. Kevill, *J. Chem. Soc., Chem. Commun.*, (1981) 421.
- [27] M. Solà, J. Mestres, R. Carbó and M. Duran, *J. Am. Chem. Soc.*, 116 (1994) 5909.
- [28] (a) R. Carbó, M. Arnau and L. Leyda, *Int. J. Quantum Chem.*, 17 (1980) 1185. (b) R. Carbó and B. Calabuig, *Int. J. Quantum Chem.*, 42 (1992) 1681.
- [29] (a) R. Carbó, B. Calabuig, L. Vera and E. Besalú, *Adv. Quantum Chem.*, 25 (1994) 253. (b) E. Besalú, R. Carbó, J. Mestres and M. Solà, in *Molecular Similarity. Topics in Current Chemistry Series*, Springer, Vol. 173, Berlin, 1995, pp. 31–62. (c) R. Carbó and E. Besalú, in R. Carbó (Ed.), *Molecular Similarity and Reactivity: From Quantum Chemistry to Phenomenological Approaches*, Kluwer, Dordrecht, 1995, pp. 3–30.
- [30] R. Carbó and Ll. Domingo, *Int. J. Quantum Chem.*, 32 (1987) 517.
- [31] (a) M. Solà, J. Mestres, M. Duran and R. Carbó, *J. Chem. Inf. Comput. Sci.*, 34 (1994) 1047. (b) J. Mestres, M. Solà, M. Duran and R. Carbó, *J. Comp. Chem.*, 15 (1994) 1113. (c) J. Mestres, M. Solà, M. Duran and R. Carbó, in R. Carbó (Ed.), *Molecular Similarity and Reactivity: From Quantum Chemistry to Phenomenological Approaches*, Kluwer, Dordrecht, 1995, pp. 89–111. (d) M. Solà, J. Mestres, R. Carbó and M. Duran, *J. Chem. Phys.*, 104 (1996) 636.
- [32] J. Mestres, M. Solà, R. Carbó, F.J. Luque and M. Orozco, *J. Phys. Chem.*, 100 (1996) 606.
- [33] (a) J. Wang, L.A. Eriksson, R.J. Boyd, Z. Shi and B.G. Johnson, *J. Phys. Chem.*, 98 (1994) 1844. (b) J. Wang, Z. Shi, R.J. Boyd and C.A. Gonzalez, *J. Phys. Chem.*, 98 (1994) 6988. (c) M. Solà, J. Mestres, R. Carbó and M. Duran, in F. Sanz, J. Giraldo and F. Manaut (Eds.), *QSAR and Molecular Modeling: Concepts, Computational Tools and Biological Applications*, Prous Science, Barcelona, 1995, pp. 403–406.
- [34] (a) R.F.W. Bader, *Acc. Chem. Res.*, 18 (1985) 9. (b) R.F.W. Bader, in *Atoms in Molecules: A Quantum Theory*, Clarendon Press, Oxford, 1990.
- [35] (a) J.S. Binkley, J.A. Pople and W.J. Hehre, *J. Am. Chem. Soc.*, 102 (1980) 939. (b) G.W. Spitznagel, T. Clark, P.v.R. Schleyer and W.J. Hehre, *J. Comput. Chem.*, 8 (1987) 1109. (c) W.J. Pietro, M.M. Francl, W.J. Hehre, D.J. DeFrees, J.A. Pople and J.S. Binkley, *J. Am. Chem. Soc.*, 104 (1982) 5039.
- [36] (a) S. Miertuš, E. Scrocco and J. Tomasi, *Chem. Phys.*, 55 (1981) 117. (b) J. Tomasi and M. Persico, *Chem. Rev.*, 94 (1994) 2027.
- [37] J. Cioslowski, *J. Am. Chem. Soc.*, 113 (1993) 6756.
- [38] M. Solà, J. Mestres, J.M. Oliva, M. Duran and R. Carbó, *Int. J. Quantum Chem.*, 58 (1996) 361.
- [39] M.J. Frisch, G.W. Trucks, H.B. Schlegel, P.M.W. Gill, B.G. Johnson, M.A. Robb, J.R. Cheeseman, T.A. Keith, G.A. Petersson, J.A. Montgomery, K. Raghavachari, M.A. Al-Laham, V.G. Zakrzewski, J.V. Ortiz, J.B. Foresman, J. Cioslowski, B.B. Stefanov, A. Nanayakkara, M. Challacombe, C.Y. Peng, P.Y. Ayala, W. Chen, M.W. Wong, J.L. Andres, E.S. Replogle, R. Gomperts, R.L. Martin, D.J. Fox, J.S. Binkley, D.J. Defrees, J. Baker, J.J.P. Stewart, M. Head-Gordon, C. Gonzalez and J.A. Pople, *GAUSSIAN 94*, Rev. A.1, Gaussian, Inc., Pittsburgh, PA, 1995.
- [40] M.W. Schmidt, K.K. Baldridge, J.A. Boatz, S.T. Elbert, M.S. Gordon, J.J. Jensen, S. Koseki, M. Matsunaga, K.A. Nguyen, S. Su, T.L. Windus, M. Dupuis, J.A. Montgomery, *J. Comput. Chem.*, 14 (1993) 1347.
- [41] D.G. Truhlar and M.S. Gordon, *Science*, 249 (1990) 491.
- [42] P. Constans and R. Carbó, *J. Chem. Inf. Comput. Sci.*, 35 (1995) 1046.
- [43] P. Constans and R. Carbó, *ASA Calculations*, Institut de Química Computacional, Universitat de Girona, Girona, CAT, 1995.
- [44] J. Mestres, *Electra*, Institut de Química Computacional, Universitat de Girona, Girona, CAT, 1994.
- [45] (a) K. Okamoto, S. Fukui and H. Shingu, *Bull. Chem. Soc. Jpn*, 40 (1967) 1920. (b) K. Okamoto, S. Fukui, I. Nitta and H. Shingu, *Bull. Chem. Soc. Jpn*, 40 (1967) 2354.
- [46] L. Pauling, *J. Am. Chem. Soc.*, 69 (1947) 542.
- [47] R.G. Pearson, *Acc. Chem. Res.*, 26 (1993) 250.